

Chemical and electrical properties of interfaces between magnesium and aluminum and *tris*-(8-hydroxy quinoline) aluminum

C. Shen and A. Kahn^{a)}

Department of Electrical Engineering and Princeton Materials Institute, Princeton University, Princeton, New Jersey 08544

J. Schwartz

Department of Chemistry, Princeton University, Princeton, New Jersey 08544

(Received 31 August 2000; accepted for publication 26 October 2000)

The chemistry, electronic structure, and electron injection characteristics at interfaces formed between *tris*-(8-hydroxy quinoline) aluminum (Alq_3) and magnesium (Mg) and aluminum (Al) are studied via x-ray photoemission spectroscopy, ultraviolet photoemission spectroscopy, and current–voltage (I – V) measurements. Both metal-on- Alq_3 and Alq_3 -on-metal interfaces are investigated. All interfaces are fabricated and tested in ultrahigh vacuum in order to eliminate extrinsic effects related to interface contamination. The propensity for Mg and Al to form covalent metal–carbon bonds leads to broad and heavily reacted interfaces when the metal is deposited on the organic film. For this deposition sequence, we propose the formation of an organometallic structure where a single metal atom attaches to the pyridyl side of the quinolate ligand of the molecule and coordinates with an oxygen atom of another ligand or of a neighboring molecule. The other deposition sequence leads to significantly more abrupt interfaces where the chemical reaction is limited to the first molecular layer in contact with the metal surface. Both types of interface exhibit chemistry-induced electronic gap states, the position of which depends on the chemical structure of the interface. The interface width, chemical structure, and electronic states appear to play no significant role in electron injection in metal/ Alq_3 /metal sandwich structures, the I – V characteristics for top and bottom injection being identical over several decades of current. © 2001 American Institute of Physics. [DOI: 10.1063/1.1333740]

I. INTRODUCTION

Metal/organic contacts continue to attract considerable interest because of their central role in the performance of organic light emitting diodes (OLEDs) and thin film transistors (OTFTs). The electrical characteristics of these contacts depend to a large extent on the energy barriers for injection of holes and electrons, which are defined as the energy difference between the Fermi level of the metal and the highest occupied molecular orbital (HOMO) or lowest unoccupied molecular orbital (LUMO) of the organic solid, respectively. Interface chemistry can also play an important role in the behavior of the contacts. Metal–molecule reactions have been shown to introduce energy levels between the metal Fermi level and the conduction level of the organic film, thereby potentially affecting the injection process. Furthermore, the diffusion of metal atoms into the organic film leads to extended interfaces, which can drastically affect the injection process. Given that the structure of thin film devices is likely to call for metal-on-organic as well as organic-on-metal interfaces, investigations of the chemistry and morphology of both types of interfaces and of their impact on the electrical properties of these interfaces are highly desirable.

The chemical structure of interfaces between *tris*-(8-hydroxyquinoline)aluminum (Alq_3) and low work function

metals, e.g., magnesium (Mg), aluminum (Al), lithium (Li), potassium (K), and calcium (Ca) has been recently experimentally and theoretically investigated.^{1–8} Alq_3 is one of the most extensively used electron transport and electroluminescent materials in OLEDs. Low work function metals are commonly used as electron injecting cathodes for this organic material. Interest in the fundamental properties of these interfaces is therefore considerable. Mg,^{1–5} Ca,^{6,8} and Li and K^{7,8} deposited on Alq_3 have been shown to donate a charge to the molecule. The theoretical investigation of Zhang *et al.*³ on Mg/ Alq_3 concludes that Mg is inserted into the central part of the molecule with no direct interaction with the Alq_3 ligands. Curioni *et al.*⁸ place Li, Al, and Ca in positions of maximum coordination with the three oxygen atoms of the facial Alq_3 isomer. Combined experimental and theoretical investigations of Li and K on Alq_3 by Johanson *et al.*⁷ propose a geometry whereby Li and K interact mostly with one ligand of the molecule and one oxygen atom of another ligand. By and large, however, these investigations ignore the possibility of the formation of an organometallic as a reaction product, in spite of the wide range of tendency for these metal atoms to form metal–carbon bonds. The experimental data presented in these various investigations show metal-deposition-induced chemical shifts of the core levels of the molecule constituents toward lower binding energy (BE) only, which supports the picture of a simple negative charge enhancement on the molecule due to charge do-

^{a)}Author to whom correspondence should be addressed; Tel: (609) 258-4642; electronic mail: kahn@ee.princeton.edu

nation by the metal atom. The data presented here demonstrate that this chemical picture is somewhat incomplete, at least for the Mg/Alq₃ and Al/Alq₃ interfaces. Using x-ray photoemission spectroscopy (XPS), we show that the O(1s) and Al(2p) core level data bring key information on the coordination of the metal adatom. We also present a comparative study of the chemistry that takes place at the metal (Mg,Al)-on-Alq₃ and Alq₃-on-metal interfaces. We observe that chemical reactions take place in both cases.

From the interface electronic structure point of view, investigations using ultraviolet photoemission spectroscopy (UPS) have shown that Li and K,⁷ Mg,^{1,2,5} and Ca (Ref. 6) deposited on Alq₃ induce filled electronic states in the gap of the organic film. Similar states have been observed at a number of interfaces involving other small molecules, such as 3,4,9,10-perylenetetracarboxylic dianhydride (PTCDA),⁹ or polymers.¹⁰ Electron-filled gap states at metal/organic interfaces can be attributed to two different mechanisms. The first is a simple metal-to-molecule charge transfer at an interface between a low work function metal and a high electron affinity organic. Charge transfer to the LUMO is energetically favorable, leading to the formation of polaron-type states. The second is the formation of a new chemical compound deriving from interface reaction, with a different electronic structure from that of the pristine molecule.

Two comments should be made regarding these states. First, the vast majority of the studies published so far associate gap states with the deposition of metal on organic, rather than organic on metal, with the chemistry and overall physical disruption taking place at such interfaces. However, our recent studies of Alq₃ on Mg^{4,5} and PTCBI on Ag and Mg (Ref. 11) demonstrate that the formation of gap states also occurs at abrupt organic-on-metal interfaces. This is confirmed in the present article for Alq₃ on Al. Although the metal-on-top and organic-on-top interfaces are structurally and chemically different, as will be seen below, common characteristics can be invoked to justify the presence of gap states at both interfaces. The second comment concerns the impact of the gap states and of the interface structure on the charge carrier injection process. Some confusion on this point resulted from an early observation of a large asymmetry in the current-voltage (*I*-*V*) characteristic on a nominally symmetric Mg:Ag/Alq₃/Mg:Ag structure.¹² The electron current injected from the electrode deposited on the organic (top electrode) was found to be 2 to 3 orders of magnitude larger than the electron current injected from the electrode on which the organic film was deposited (bottom electrode). The prevalent mode of thinking derived from these observations, and later reinforced by investigations of top indium tin oxide electrodes sputter-deposited on CuPc,¹³ was that the chemical and morphological disruption caused by the deposition of the hot and reactive metal atoms on the soft organic film did lower the resistivity of the contact to the organic layer. However, a reevaluation of the electrical behavior of Mg:Ag/Alq₃/Ag:Mg structure fabricated in ultrahigh vacuum recently led to the conclusion that the *I*-*V* characteristics were totally symmetric over several decades of current,⁴ and that the current asymmetry previously ob-

served was an extrinsic effect due to the formation of a thin oxide layer on the bottom electrode in poor vacuum.

These various issues are clearly of paramount importance for the fabrication of organic devices in which both metal-on-top and organic-on-top interfaces are present. Beyond the basic problem of the choice of materials, they pertain to the fabrication environment and device processing. The chemistry and electronic structure of these interfaces demand therefore in-depth investigations. Our work makes use of ultrahigh vacuum techniques (for film deposition, interface measurements, and electrical testing) in order to eliminate extrinsic interface effects due to contamination and focus on the fundamental processes only. We confirm that the fabrication of Mg(Al)/Alq₃/Mg(Al) structures in ultrahigh vacuum lead to symmetric top and bottom injection characteristics. We show that gap states are induced at both metal-on-organic and organic-on-metal interfaces, although the spatial extent of gap state formation is different due to different levels of diffusion of metal atoms into Alq₃. The relationship between physical and chemical properties of the interfaces and the carrier injection is discussed.

II. EXPERIMENT

The experiments were performed in an ultrahigh vacuum system composed of three interconnected chambers equipped for surface preparation, film growth, and analysis. The Alq₃ and metal films were deposited via thermal evaporation on substrates consisting of Au(500 Å)/Cr(250 Å)/Si. All evaporations were done in the growth chamber at a base pressure lower than 1×10^{-9} Torr. XPS was used to verify the absence of surface contamination, i.e., by O or C, on the metal films grown under these conditions.

The sample structure for the metal-on-Alq₃ interface studies was a 100 Å thick organic layer deposited on the Au substrate, on which the metal layer was incrementally deposited. For Alq₃-on-metal, the base was a 500 Å Mg or Al layer on top of which the organic layer was incrementally deposited. In both cases, UPS spectra of the pristine starting surface were recorded. XPS and UPS spectra were recorded in the analysis chamber (base pressure = 5×10^{-11} Torr) in two separate experiments to eliminate possible deleterious effects of x-rays on the electronic structure of the organic layer. Mg(2p), Al(2p), C(1s), N(1s), and O(1s) core levels were recorded using the Zr M_ζ (151.4 eV) or the Al K_α (1486.6 eV) photon lines of our x-ray source. The valence states were recorded using the He I (21.2 eV) and He II (40.8 eV) radiation lines from a gas discharge lamp. The resolution of the XPS and UPS measurement was 0.7 and 0.1 eV, respectively. Finally, metal/Alq₃/metal structures consisting of a 500 Å metal base, a 1200 Å Alq₃ layer, and a 700 Å top metal electrode evaporated through a shadow mask with arrays of 0.78, 0.13, and 0.078 mm² round apertures were made in the growth chamber. These samples were then transferred to the preparation chamber for *I*-*V* measurement in 5×10^{-10} Torr vacuum.

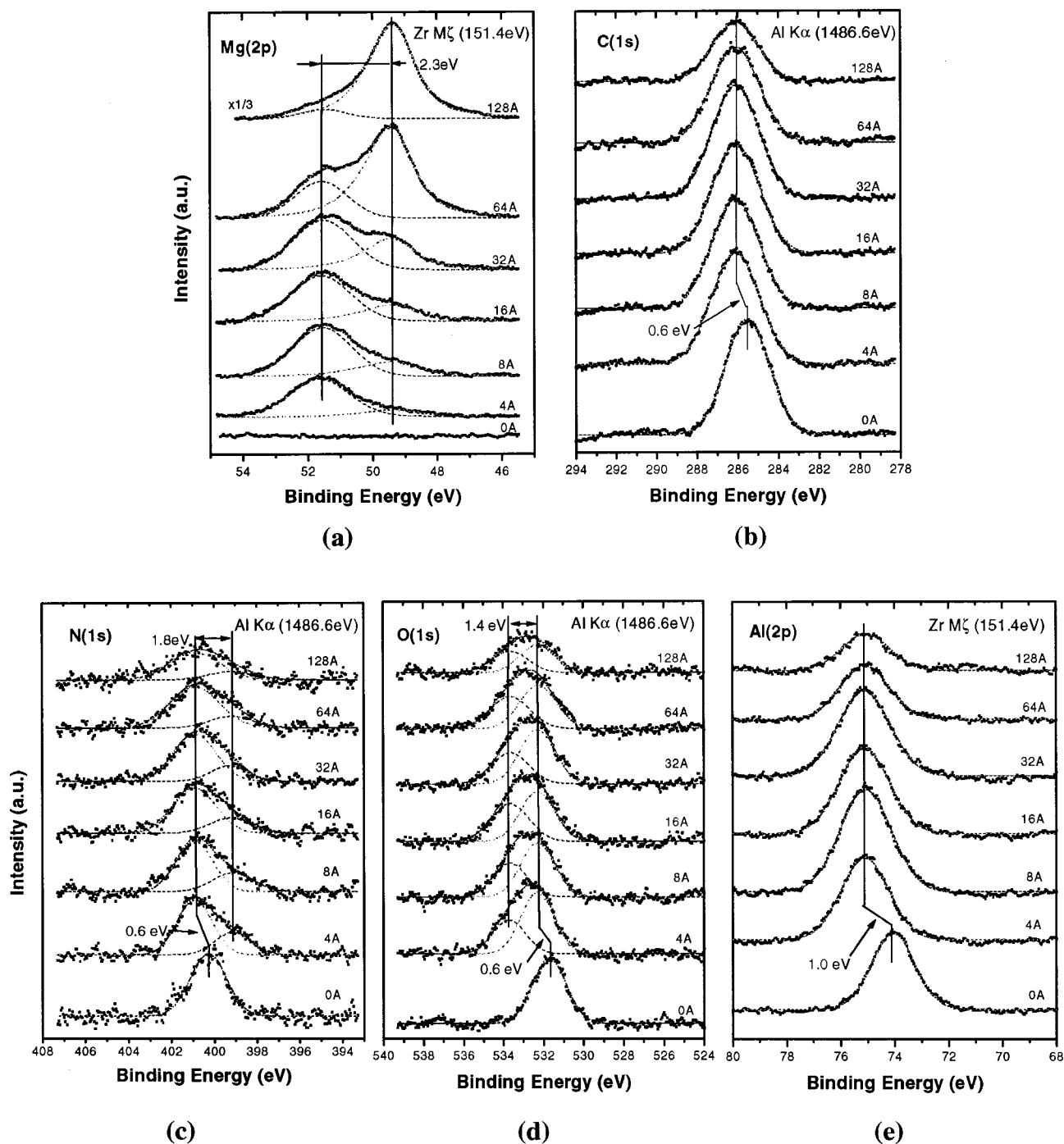


FIG. 1. (a) Mg(2*p*), (b) C(1*s*), (c) N(1*s*), (d) O(1*s*), and (e) Al(2*p*) core levels measured as a function of Mg coverage on Alq₃.

III. RESULTS

A. Metal-on-Alq₃ interfaces

The evolution of the Mg(2*p*), C(1*s*), N(1*s*), O(1*s*), and Al(2*p*) core level peaks as a function of Mg coverage on Alq₃ is shown in Figs. 1(a)–1(e). Following the initial deposition (4 Å), the Mg(2*p*) peak consists mostly of a high BE component at 51.6 eV, while a small low BE component appears at 49.3 eV [Fig. 1(a)]. The 0.4 eV spin-orbit splitting of Mg(2*p*) is not resolved in this experiment, and each component is fitted with a single Gaussian function. With increasing Mg coverage, the low BE component grows and

dominates the spectrum for nominal coverages beyond 32 Å. This component corresponds to metallic Mg that accumulates on top of the organic film at high coverage, while the high BE component represents strongly oxidized Mg that has donated a charge to the molecule. The C(1*s*) core level undergoes a 0.6 eV shift to higher BE with the first Mg deposition [Fig. 1(b)], and remains at the same energy thereafter. The same shift is observed on the N(1*s*) and O(1*s*) core level, and represents a rigid shift analogous to band bending induced by the deposition of a metal on an inorganic semiconductor surface. The full width at half maximum (FWHM)

of the C(1s) peak remains approximately constant at 2.6 eV, with an increase of less than ~ 0.2 eV with Mg deposition. However, the N(1s) and O(1s) peaks broaden considerably. The Mg deposition induces a low BE N(1s) component at 399.1 eV that corresponds to an excess electronic charge on and around N [Fig. 1(c)]. The chemical shift is ~ 1.8 eV. More surprisingly, the Mg deposition leads to the formation of a high BE component of the O(1s) core level [Fig. 1(d)]. The 1.4 eV chemical shift corresponds to a net withdrawal of negative charge from oxygen. Finally, the Al(2p) undergoes a 1 eV shift to higher BE, which corresponds to a net chemical shift of 0.4 eV to higher BE over and beyond the ubiquitous 0.6 eV "band bending" shift. The peak areas of the O(1s), C(1s), N(1s), and Al(2p) remain basically unchanged up to a nominal coverage of 32 Å, indicating that Mg does not accumulate on the surface of the organic film in that coverage range. While this is partly due to the low sticking coefficient of Mg on Alq₃, the increase in the total area of the Mg(2p) peak demonstrates that the overall metal atom concentration does increase, and thus indicates that the metal atoms penetrate into the film. Eventually, reaction sites are depleted, Mg atoms begin to accumulate at the surface, and the intensity of the various Alq₃ signals is attenuated.

Figures 2(a)–2(d) show the evolution of Al(2p), C(1s), N(1s), and O(1s) core levels as a function of Al coverage on Alq₃. The Al(2p) spectrum consists of several components, presumably Al in unreacted and reacted molecules, metallic Al, reacted Al, and perhaps unreacted Al which has diffused into the organic matrix. A detailed analysis via peak decomposition is therefore extremely difficult and will not be attempted here. However, the low and high coverage cases are quite clear, with the 2 Å Al spectrum corresponding mainly to reacted Al, and the 32 Å spectrum dominated by the metallic component. It is clear from the rapid increase in the Al(2p) peak area that, unlike Mg, Al sticks to the organic film. More important, and similar to the previous case, the N(1s) spectrum shows a low BE component shifted by 1.8 eV, while the O(1s) spectrum shows a high BE component shifted by ~ 1.4 eV. The similarities between these results and those of the Mg/Alq₃ case suggest a similar metal-molecule reaction. There is also a slight shift (~ 0.2 eV) of all the Alq₃ core levels to lower BE at 16 Å Al coverage and above. Finally, the C(1s) FWHM increases only by ~ 0.2 eV with Al deposition.

The UPS spectra of the upper valence states of Mg/Alq₃ [Fig. 3(a)] are in excellent agreement with previously published data.^{1,2} Two angstroms of Mg attenuate the Alq₃ features, although the molecular peaks remain clearly identifiable. All the molecular levels shift by 0.6 eV toward higher BE and remain at the same energy thereafter, in good agreement with the 0.6 eV shift noted for all the core levels mentioned above. Mg induces a state at ~ 1.9 eV above the original HOMO in the gap of Alq₃. The UPS spectrum remains basically unchanged upon further Mg deposition. A weak Mg Fermi edge becomes visible only above a nominal thickness of 64 Å. Mg is known for its poor sticking coefficient on many materials. While it is possible that Mg does not stick well to Alq₃, results presented above demonstrated that Mg does accumulate with increasing deposition. Therefore

the absence of a Mg Fermi edge at the surface is partly attributed to chemical reaction and Mg diffusion into the film in the early stages of deposition.

Figure 3(b) shows the upper valence states of Al/Alq₃. One monolayer of Al atoms attenuates the Alq₃ features significantly, indicating extensive chemical reaction. A gap state at ~ 1.6 eV above the original HOMO is identified at 0.5 Å of Al deposition. The Al Fermi edge appears for a coverage of 16 Å, in accord with the higher sticking coefficient noted above. Finally, there is a 0.2 eV shift of the valence states to higher BE at 0.5 Å of Al deposition. Surprisingly, this shift is not observed in the Alq₃ core levels. We attribute this discrepancy to the different initial work functions of the substrates used in the XPS and UPS experiments.

B. Alq₃-on-metal interfaces

Figures 4(a)–4(e) show the evolutions of the Mg(2p), C(1s), N(1s), O(1s), and Al(2p) core levels for the deposition of Alq₃ on Mg. Following the initial Alq₃ deposition, a high BE Mg(2p) component develops at 51.1 eV [Fig. 4(a)]. The relative contribution of this component remains small throughout the coverage range, indicating that its origin is confined to the organic/metal interface region. The chemical shift with respect to the metallic component is 1.8 eV (versus 2.3 eV for Mg-on-Alq₃), suggesting a reduced charge exchange per Mg atom involved in the process. The interface C(1s) broadens substantially in this deposition sequence as evidenced by the low coverage FWHM, which is 0.5 eV wider than for bulk Alq₃ [Fig. 4(b)]. The peak position is at a ~ 0.3 eV lower BE position with respect to that of the bulk C(1s). The same 0.3 eV shift is observed in other core level spectra. The low photoionization cross section of N(1s) and the initial superposition of a Mg KL₁L₁ Auger peak render the detection of N difficult at low coverage. However, after the subtraction of the Mg KL₁L₁ Auger peak, the data indicate the presence of a component shifted to lower BE by ~ 1.9 eV (versus 1.8 eV for Mg-on-Alq₃) with respect to the main Alq₃ peak [Fig. 4(c)]. For the O(1s) core level, two components can clearly be distinguished, the interface component being shifted to higher BE by ~ 1.2 eV (versus 1.4 eV for Mg-on-Alq₃) with respect to the main Alq₃ peak. For the Al(2p) core level, the interface component is shifted toward higher BE by 0.2 eV (versus 0.4 eV for Mg-on-Alq₃) with respect to the bulk component. The same sign of chemical shifts suggest therefore a chemical reaction similar to that obtained for Mg-on-Alq₃. The quantitative difference in the shifts and relative peak areas, however, suggest some difference in the level of interaction. The Mg(2p) peak area decreases approximately exponentially with Alq₃ coverage, leading to a calculated electron attenuation length of 16 ± 2 Å at an electron kinetic energy of ~ 97 eV. The Alq₃ coverage on Mg appears therefore to be uniform, although some clustering cannot be ruled out. This result is consistent with our UPS study that indicates that 16 Å of Alq₃ completely covers the Mg surface.

Figures 5(a)–5(d) show the evolution of Al(2p), C(1s), N(1s), and O(1s) core levels for the deposition of Alq₃ on

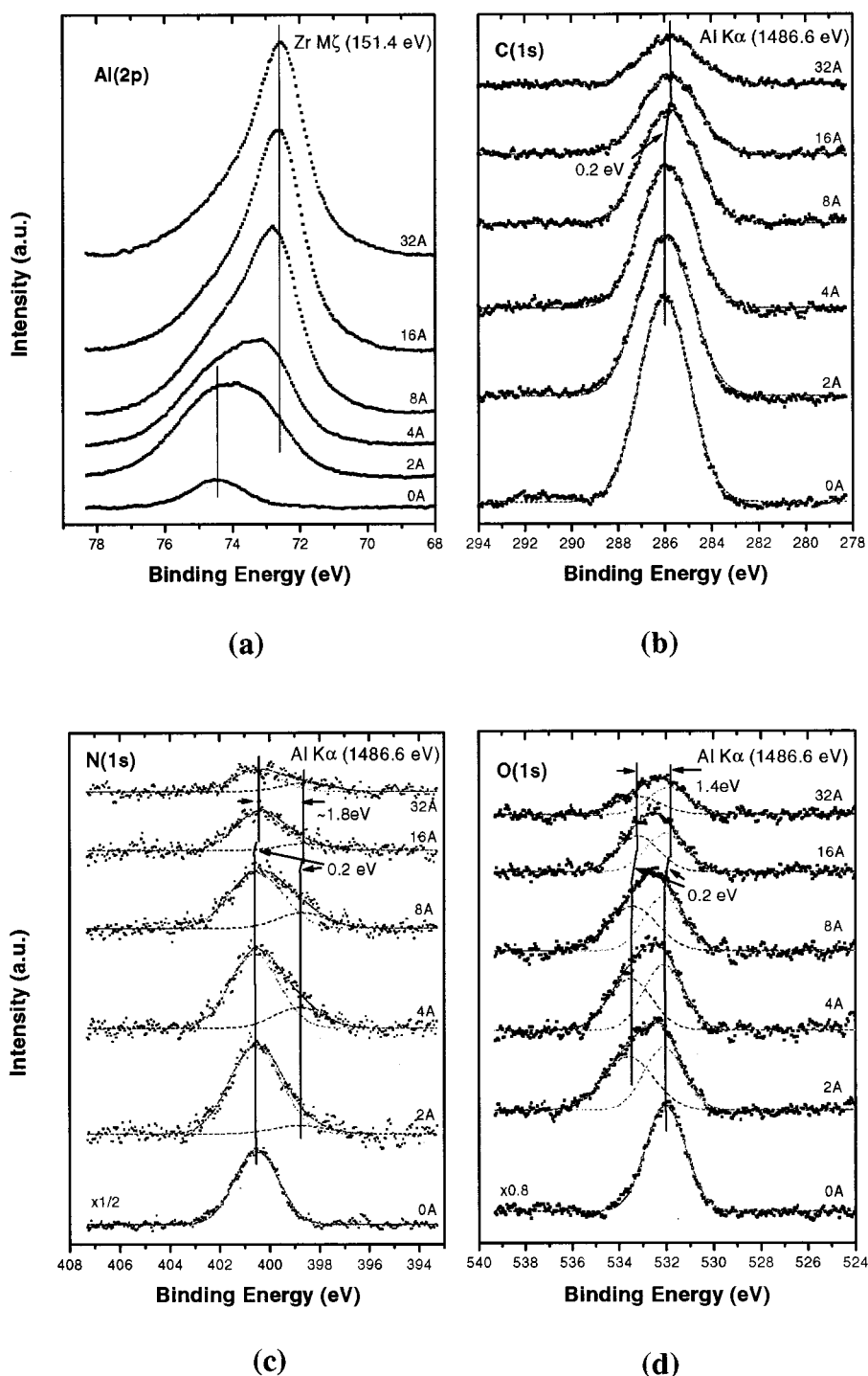


FIG. 2. (a) Al(2*p*), (b) C(1*s*), (c) N(1*s*), and (d) O(1*s*) core levels measured as a function of Al coverage on AlQ₃.

Al. As explained above, the Al(2*p*) spectrum is difficult to analyze because multiple species are involved. However, the metallic component is clearly resolved. Its exponential decrease as a function of molecular coverage leads to an electron attenuation length of 9 ± 1 Å for an electron kinetic energy of ~ 75 eV, which indicates a more homogeneous coverage of the metal surface than in the previous case. Similar to the case of AlQ₃-on-Mg, the FWHM of C(1*s*) is broadened at the interface by ~ 0.5 eV and shifted by ~ 0.3 eV toward lower BE. The N(1*s*) core level exhibits a ~ 2.0

eV (versus 1.8 eV for Al-on-AlQ₃) lower BE component at the interface, while O(1*s*) exhibits a ~ 0.7 eV (versus 1.4 eV for Al-on-AlQ₃) higher BE component.

The UPS spectra corresponding to the deposition of AlQ₃ on Mg are shown in Fig. 6(a). The data are consistent with a homogeneous coverage of the substrate by the organic film. The 16 Å spectrum is almost identical to that of a thick AlQ₃ film, in accordance with the formation of an abrupt interface. However, contrary to previous measurements,¹ the low coverage spectra show a gap state at ~ 1.6 eV above the initial

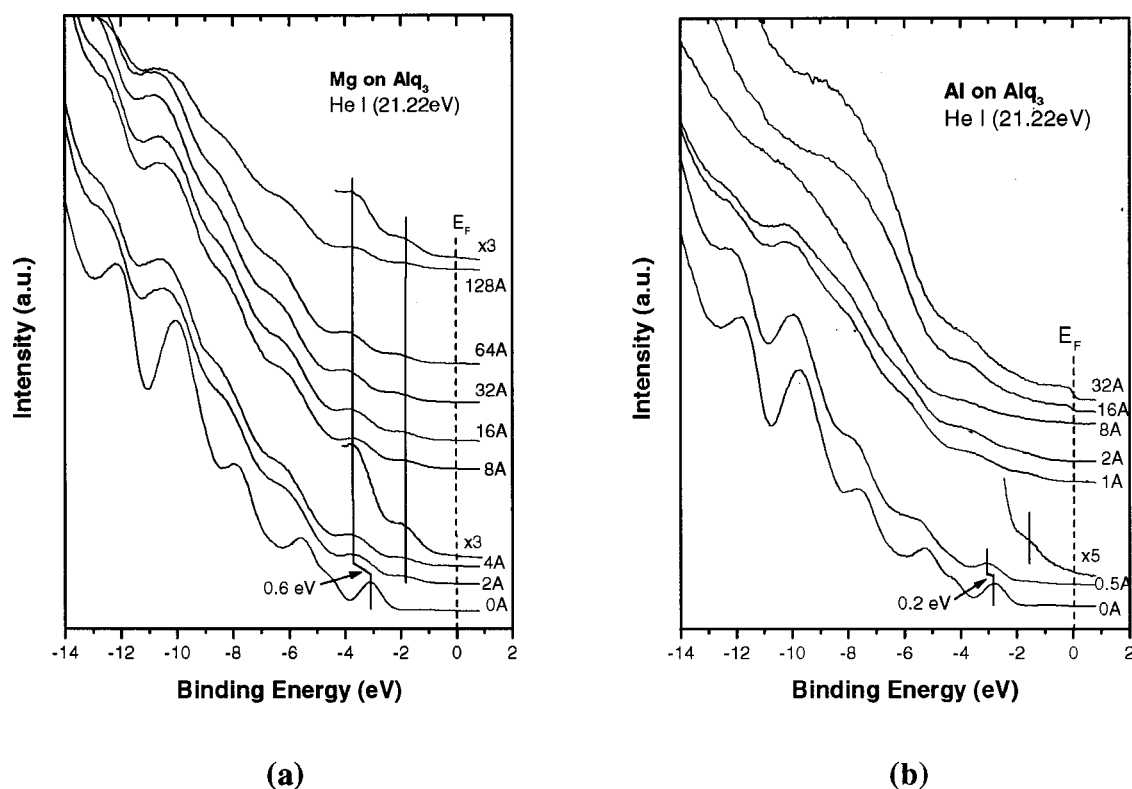


FIG. 3. UPS valence spectra measured as a function of (a) increasing Mg coverage on Alq_3 and (b) increasing Al coverage on Alq_3 .

HOMO, similar to that resulting from the metal-on-organic deposition. In addition to this gap state, peaks at -10 and -11 eV, which are not seen on the thick Alq_3 spectrum, are detected near the interface, suggestive of a chemical interaction between the first molecular layer and the substrate. Figure 6(b) shows the UPS spectra corresponding to the deposition of Alq_3 on Al. A gap state at ~ 1.9 eV above the initial HOMO is clearly observed. The 16 \AA spectrum is in good agreement with that of bulk Alq_3 , indicating that less than two monolayers of Alq_3 are sufficient to entirely cover the Al substrate.

Finally, and very important from the point of view of injection barriers, the energy difference between the Fermi level and the Alq_3 HOMO is identical at the metal-on- Alq_3 and Alq_3 -on-metal interfaces. The values are 2.8 eV for Mg/Alq_3 and 2.5 eV for Al/Alq_3 .

C. Current–voltage measurements

Figure 7 shows the room temperature I – V characteristics measured *in situ* for (a) $\text{Mg}/\text{Alq}_3/\text{Mg}$, (b) $\text{Mg}:\text{Ag}/\text{Alq}_3/\text{Mg}:\text{Ag}$, and (c) $\text{Al}/\text{Alq}_3/\text{Al}$. In these measurements, the forward bias current corresponds to electrons injected from the metal-on- Alq_3 contact, whereas the reverse bias current corresponds to electrons injected from the Alq_3 -on-metal contact. The forward and reverse I – V characteristics are highly symmetric in all three cases.

IV. DISCUSSION

The XPS data suggest similar structures for the two metal-on-top interfaces on the one hand, and for the two

Alq_3 -on-top interfaces on the other. The key pieces of information are the chemical shifts of the $\text{O}(1s)$ and $\text{Al}(2p)$ core levels toward higher BE. The sign of these chemical shifts, which is opposite to that of the $\text{N}(1s)$ component, is incompatible with a simple charge donation from the metal atom to the molecule, and signals the formation of an organometallic complex. In that regard, the propensity to form metal–C, and the strength of metal–O bonds varies greatly among the metal atoms discussed in the introduction. We can therefore expect fundamental differences in the reaction products derived from the deposition on Alq_3 of Al and Mg on the one hand, K or Ca on the other.

Relative tendencies for C–metal covalent bonding have been discussed¹⁴ in terms of relative charge/radius ratios, based on ionic radii of the metallic cations, which can be expressed,¹⁵ as well, in terms of charge density (Table I). Our model⁵ is based on these data and by analogy with the reaction of Mg with anthracene, which gives a covalently bonded organomagnesium adduct.^{16,17} Thus Mg deposited on Alq_3 is suggested to react at the pyridyl ring of the quinolate ligand by covalent bond formation (Fig. 8). Overall, the Mg is oxidized by donation of charge to the Alq_3 LUMO, which is maximized on the pyridyl ring and at N.¹⁸ The resulting negative charge buildup on the ligand, along with some rehybridization at N from sp^2 to sp^3 , result in a lowering of the BE of the $\text{N}(1s)$ core level. The Mg ion should be out of the plane of the quinolate ligand (the *ipso* carbon in Mg anthracene is rehybridized^{17,19} to sp^3), and can coordinate as an electrophile to a quinolate O intramolecularly (or perhaps intermolecularly), which reduces the donor ability of that O

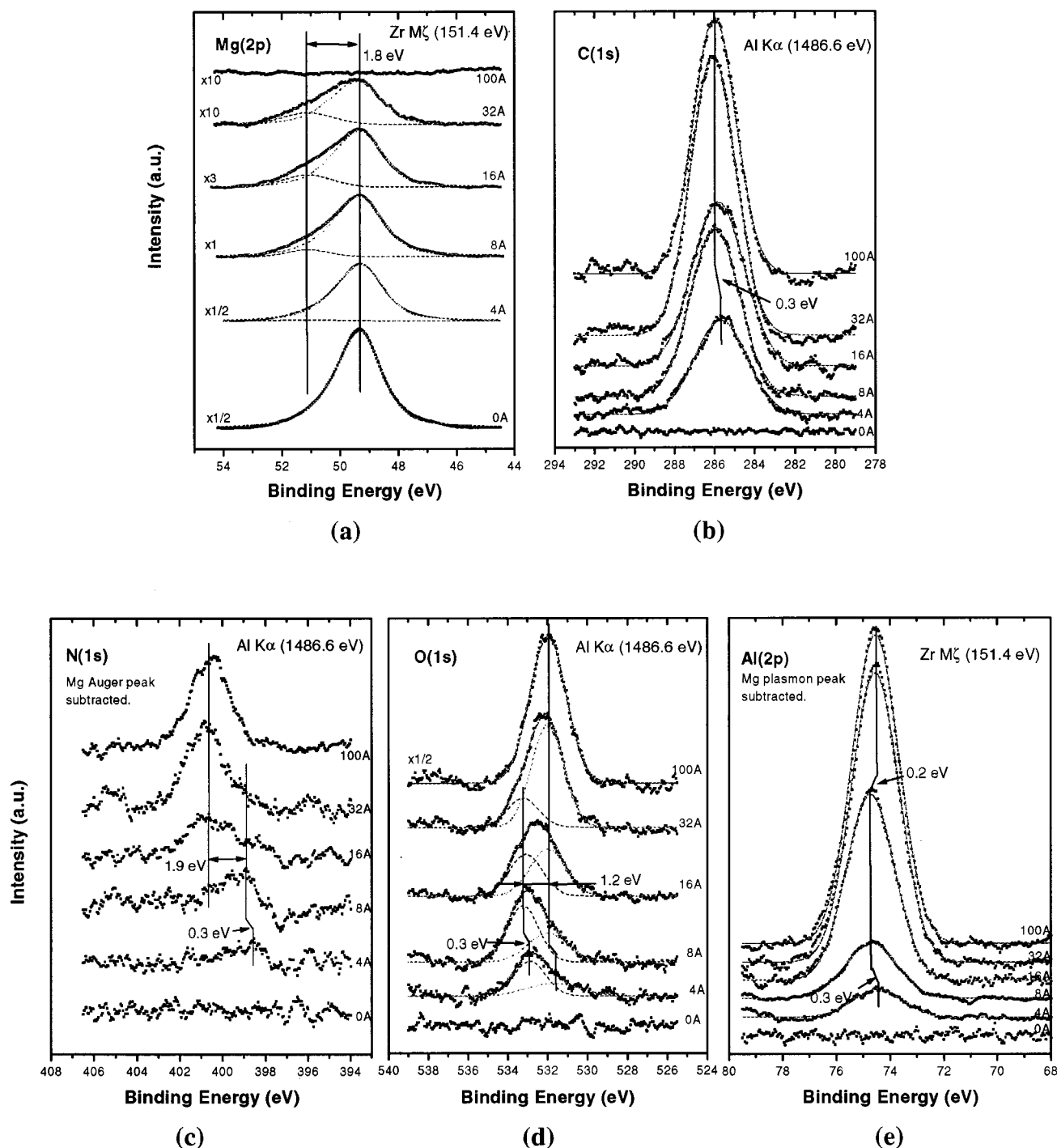


FIG. 4. (a) Mg(2p), (b) C(1s), (c) N(1s), (d) O(1s), and (e) Al(2p) core levels measured as a function of Alq₃ coverage on Mg.

with regard to the central Al atom of the Alq₃ molecule. Accordingly, the observed chemical shift changes, by 1.8 eV for O(1s) and by 0.4 eV for Al(2p), to higher binding energies can be explained: Mg metal reacts with Alq₃ to give a product whose structure is consistent with expectations for strong Mg bonding to both O and C, and is inconsistent with the ion pairing model proposed by Curioni *et al.*⁸ Al, too, would be expected to form C–Al σ -bonds²⁰ on reaction with Alq₃. Indeed an Al adduct of Mg anthracene does involve C–Al σ -bonding,²¹ as does the Al adduct with benzene, as determined both by theoretical²² and spectroscopic studies.²³

Ca and K, on the other hand, would be expected to form ion pairs with an organic ligand radical anion or dianion and to coordinate with O, but weakly (the Li, Ca, and K analogs of Mg anthracene are in fact ion pairs).^{24–26} These expectations are consistent with XPS chemical shifts observed experimentally for the Ca–Alq₃ system.⁶

In the case of Alq₃ deposited on Mg or Al, the XPS data are consistent with the formation of an abrupt interface with chemical interaction and charge exchange limited to the first or second interfacial molecular layer. The charge donated by a metal atom to a molecule is partly compensated by the

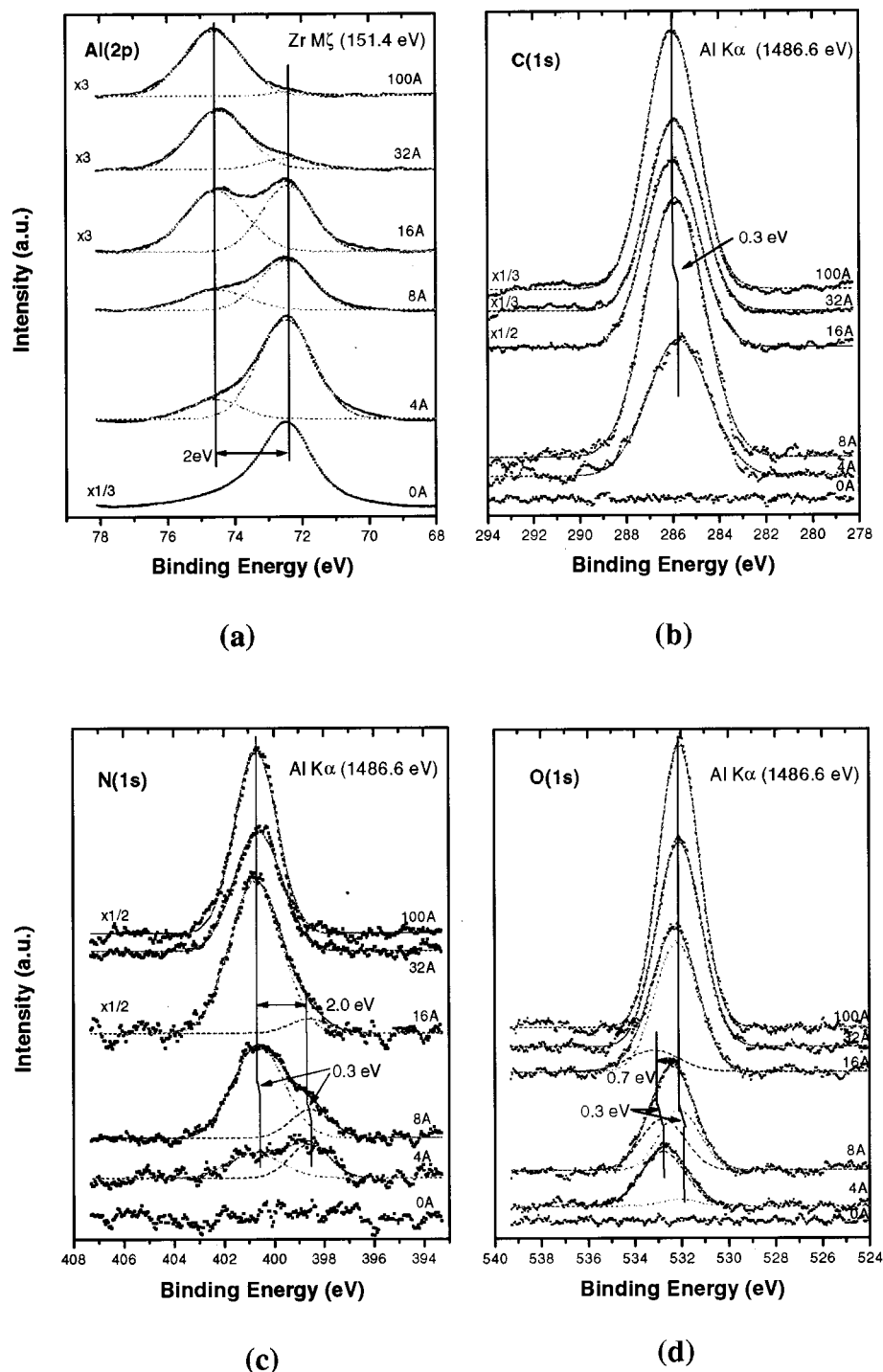


FIG. 5. (a) Al(2p), (b) C(1s), (c) N(1s), and (d) O(1s) core levels measured as a function of AlQ₃ coverage on Al.

abundant reservoir of electrons in the metal. The chemical shift of the oxidized metal species is therefore smaller than that obtained at the corresponding metal-on-AlQ₃ interface (e.g., 1.8 versus 2.3 eV for Mg). Furthermore, the N(1s) chemical shift toward lower BE is larger, and the O(1s) and Al(2p) chemical shifts toward higher BE are smaller, than the corresponding shifts found for the metal-on-top interface. These core level shifts originate from two opposite effects: (i) the charge transfer from the metal atom to the molecule, which shifts all levels toward lower BE and (ii) the coordi-

nation of the metal atom with the molecule, which pulls charge away from the molecule and shifts the levels toward higher BE. Here, the metal atoms are bound in the metal lattice in a lower energy state than single metal atoms. The chemical bonds between AlQ₃ and these metal atoms are therefore weaker than for the other interface. As a result, the charge pulled back from the molecule is smaller and the negative charge distributed on the molecule is larger. The chemically shifted N(1s) component therefore appears at a lower BE as compared to its counterpart at the metal-on-AlQ₃

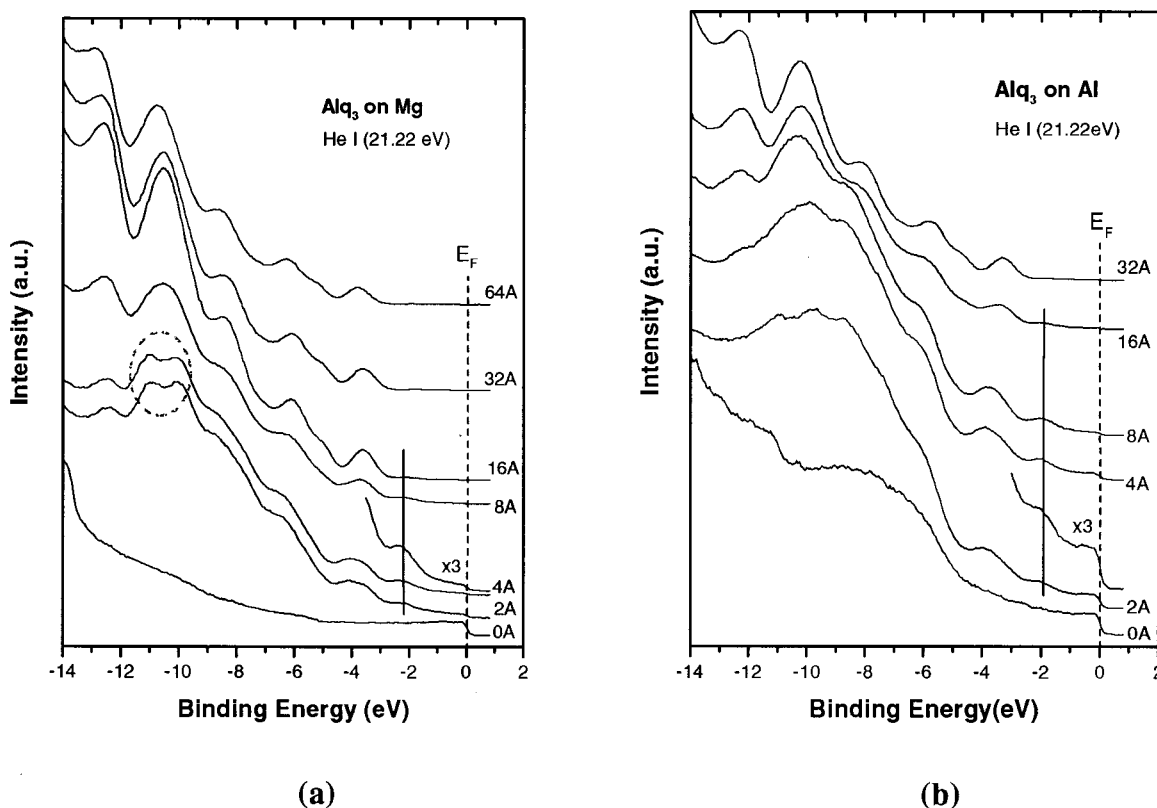


FIG. 6. UPS valence spectra measured as a function of (a) increasing Alq₃ coverage on Mg and (b) increasing Alq₃ coverage on Al.

interfaces, and the chemical shifts toward higher BE of the O(1s) and Al(2p) components, which result from charge withdrawing due to metal–molecule coordination, are smaller.

An effect that should be noted from Figs. 4(b) and 5(b) is the broadening of the C(1s) FWHM at the Alq₃-on-metal interfaces. Chemical reaction with surface metal atoms is a source of broadening. However, a much smaller broadening

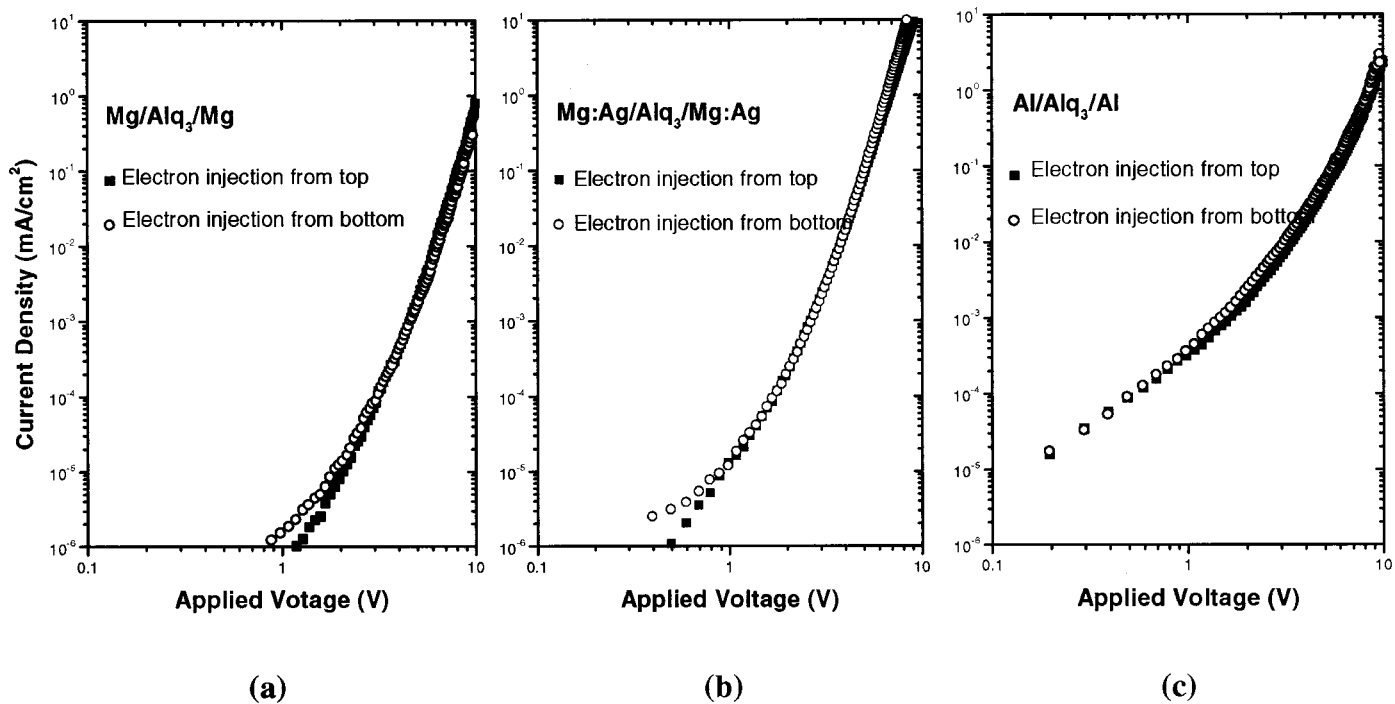


FIG. 7. Forward and reverse current versus voltage characteristics measured for the symmetric (a) Mg/Alq₃/Mg, (b) Mg:Ag/Alq₃/Mg:Ag, and (c) Al/Alq₃/Al structures.

TABLE I. Charge densities for several metallic species.

Metallic species	Charge density ^a
Ti ⁴⁺	362
Al ³⁺	770 (tetrahedral); 364
Mg ²⁺	120
Li ⁺	98 (tetrahedral); 52
Na ⁺	24
K ⁺	11
Ca ²⁺	52

^aDefined as ionic charge per unit of volume (all species are assumed to be 6-coordinate, unless otherwise indicated).

is observed at the metal-on-top interfaces where the metal-molecule reaction is stronger. Inhomogeneous polarization is another source of broadening. The polarization of the molecule is known to depend sensitively on the surrounding environment. At low Alq₃ coverage, the organic film likely consists of molecules (i) scattered isolated on the surface, (ii) positioned in a monolayer film on the metal surface, and (iii) surrounded by other molecules in small three-dimensional clusters. The polarization of the core hole created in the photoemission process is therefore likely to be inhomogeneous, leading to the observed FWHM broadening. On the other hand, the molecular environment at the initial stages of deposition of metal on the 100 Å Alq₃ film is more homogeneous, and does not give rise to any significant polarization-induced broadening. This effect is seen predominantly on the C(1s) level, all other species of the molecules having chemically shifted core level components that mask this effect. Finally, the shift of all core levels toward higher BE away from the interface is strongly suggestive of final state effects due to diminishing screening of the core hole by the metal. The screening effect is also observed at the Al-on-Alq₃ interface. All Alq₃ core levels shift to lower BE by 0.2 eV at 16 Å Al coverage and above. The shifts are not observed at Mg-on-Alq₃ up to 128 Å of Mg coverage. This is consistent with our UPS study that shows no Fermi edge at increasing Mg coverage. Metal screening is therefore insufficient. In our UPS study on Alq₃/metal, the screening effect is reflected in the higher ionization energy of Alq₃ near the Alq₃/metal interface.

The spatial extent of the chemical reaction and diffusion is different at the metal-on-top and organic-on-top interfaces. The UPS and XPS data show that the first few angstroms of Mg or Al atoms deposited on Alq₃ do not accumulate on the organic surface. The adatoms diffuse into the film. The Alq₃ UPS features are significantly attenuated by the deposition of

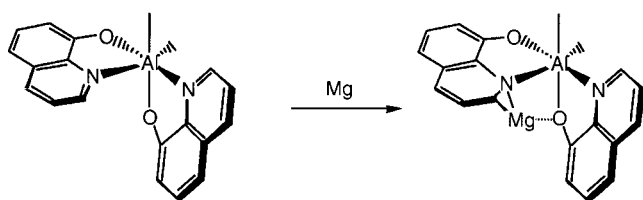


FIG. 8. Structural representation of the interface structure due to the formation of an organometallic complex.

~2 Å of Mg or Al. We stress here that 2 Å of metal contain a number of atoms sufficient to react with about ten molecular layers of Alq₃, assuming that each metal atom reacts with one organic molecule. Most of the observable chemistry takes place during the very early stages of deposition. Further deposition leads to diffusion of metal atoms into the organic film, then to the accumulation of metal on the surface for nominal coverages beyond 4 Å. We can therefore estimate that the metal-on-Alq₃ interfaces are reacted over ten molecular layers, in contrast to the Alq₃-on-metal interfaces where chemistry is observed at the level of the first molecular layer of Alq₃ only. UPS spectra of 16 Å Alq₃ (~2 molecular layers) on metal show “bulk-like” Alq₃ UPS features, demonstrating the abruptness of the interface.

The final point to be addressed concerns the impact of the deposition sequence on the electron injection process. Both types of interfaces include electronic gap states above the Alq₃ HOMO (Figs. 3 and 6), which correspond to the electronic structure of the reaction product at the interface. The difference in energy position of these states (with respect to the HOMO) at the metal-on-organic and organic-on-metal interfaces is attributed to the different bonding configurations and charge transferred between the molecule and the isolated metal adatom in one case, and the metal surface in the other.

The identical forward and reverse *I*-*V* characteristics of Fig. 7 show that the morphological and chemical differences between the two interfaces have little, if any, impact on the carrier injection properties. This is consistent with the fact that the HOMO-to-Fermi level energy difference given at the end of Sec. III B indicates that the electron injection barriers at the organic-on-metal and metal-on-organic interfaces are identical. The interesting point is that the metal-on-organic and organic-on-metal interfaces lead to identical *I*-*V* characteristics (Fig. 7) in spite of the demonstrated difference in metal penetration and interface abruptness. Indeed, it was believed that a depth distribution of the type of gap states observed at the interfaces would facilitate current injection, via a “stepping stone” effect,¹³ thereby leading to a higher injection current from the metal on top interface. The present data clearly suggest otherwise. We know that previously observed current asymmetries at Mg:Ag/Alq₃/Mg:Ag structures¹² were due to electrode contamination effects and were not related to intrinsic differences between the two interfaces.⁴ Another factor contributing to the symmetric behavior of these structurally asymmetric interfaces may be that the degree of asymmetry, i.e., the penetration of Mg or Al in Alq₃ is in fact relatively small, e.g., 3 to 4 molecular layers only, thus leading to negligible interface grading effects.

Finally the current density in the Al/Alq₃/Al structure is slightly larger than that in the Mg/Alq₃/Mg structure. Mg:Ag electrodes lead to improved electron injection, as is now well-established from device performance. The difference is not really understood. We note that the error bar in the absolute current measurement can be one order of magnitude, while the symmetry or asymmetry characteristics of the *I*-*V* measurements are highly repeatable.

V. SUMMARY

We have used core level and valence state photoemission spectroscopy and current–voltage measurements to investigate the chemical structure, electronic structure, and electron injection characteristics at metal (Al,Mg)/Alq₃ interfaces. We have shown that Alq₃ undergoes a strong chemical interaction with Mg or Al. The strong shift toward higher binding energy at the ligand oxygen and the central Al atom of the molecule upon interface formation is explained using a simple organometallic model. In addition, diffusion of the metal atoms into the organic film broadens the metal-on-organic interface with respect to the organic-on-metal interface, although the extent of this broadening is unknown. Both types of interfaces exhibit a new electronic state above the HOMO in the Alq₃ gap. These states presumably correspond to the electronic structure of the organometallic compound. The electron injection barrier is found to be 0.3 eV smaller at the Mg/Alq₃ interface than at the Al/Alq₃ interface. Finally, unlike previously believed, the current injection characteristics of metal-on-top and organic-on-top interfaces are identical in spite of the structural differences noticed at the two types of interfaces. Whether the depth of metal penetration at the metal-on-top interface is insufficient to promote an increase in current injection is unknown at this point and needs to be further investigated.

ACKNOWLEDGMENTS

Support of this work by the MRSEC program of the NSF (Grant No. DMR-9809483), by the Chemistry Division of the NSF (Grant No. CHE-9901224), and by the New Jersey Center for Optoelectronics (Grant No. 97-2890-051-17) is gratefully acknowledged.

¹A. Rajagopal and A. Kahn, J. Appl. Phys. **84**, 355 (1998).

²S. T. Lee, X. Y. Hou, M. G. Mason, and C. W. Tang, Appl. Phys. Lett. **72**, 1593 (1998).

³R. Q. Zhang, X. Y. Hou, and S. T. Lee, Appl. Phys. Lett. **74**, 1612 (1999).

⁴C. Shen, I. G. Hill, and A. Kahn, Adv. Mater. **11**, 1523 (1999).

⁵C. Shen, I. G. Hill, A. Kahn, and J. Schwartz, J. Am. Chem. Soc. **122**, 5391 (2000).

⁶V.-E. Choong, M. G. Mason, C. W. Tang, and Y. Gao, Appl. Phys. Lett. **72**, 2689 (1998).

⁷N. Johanson, T. Osada, S. Stafström, W. R. Salaneck, V. Parente, D. A. dos Santos, X. Crispin, and J. L. Brédas, J. Chem. Phys. **111**, 2157 (1999).

⁸A. Curioni and W. Andreoni, J. Am. Chem. Soc. **121**, 8216 (1999).

⁹Y. Hirose, A. Kahn, V. Aristov, P. Soukiassian, V. Bulovic, and S. R. Forrest, Phys. Rev. B **54**, 13748 (1996).

¹⁰W. R. Salaneck, S. Stafström, and J.-L. Brédas, in *Conjugated Polymer Surfaces and Interfaces* (Cambridge University, Cambridge, England, 1996).

¹¹I. G. Hill, J. Schwartz, and A. Kahn (accepted for publication).

¹²V. Bulović, Ph.D. thesis, Princeton University, 1998.

¹³G. Parthasarathy, P. E. Burrows, V. Khalfin, V. G. Kozlov, and S. R. Forrest, Appl. Phys. Lett. **72**, 2138 (1998).

¹⁴W. E. Lindsell, in *Comprehensive Organometallic Chemistry II*, edited by E. W. Abel, F. G. A. Stone, and G. Wilkinson (Elsevier, Oxford, 1995), Vol. 1, Sect. 3.3.

¹⁵See, for example, G. Rayner-Canham, *Descriptive Inorganic Chemistry*, 2nd ed. (Freeman, New York, 1999), Appendix 4.

¹⁶B. Bogdanović, Acc. Chem. Res. **21**, 261 (1988).

¹⁷L. M. Engelhardt, S. Harvey, C. L. Raston, and A. H. White, J. Organomet. Chem. **341**, 39 (1988).

¹⁸I. G. Hill, A. Kahn, J. Cornill, D. A. dos Santos, and J. L. Brédas, Chem. Phys. Lett. **317**, 444 (2000).

¹⁹W. M. Brooks, C. L. Raston, R. E. Sue, F. J. Lincoln, and J. J. McGinnity, Organometallics **10**, 2098 (1991).

²⁰J. J. Eisch, in *Comprehensive Organometallic Chemistry II*, edited by E. W. Abel, F. G. A. Stone, and G. Wilkinson (Elsevier, Oxford, 1995), Vol. 1, Chap. 10.

²¹H. Lehmkuhl, K. Mehler, R. Benn, A. Rufin ska, G. Schroth, and C. Krüger, Chem. Ber. **117**, 389 (1984).

²²S. J. Silva and J. D. Head, J. Am. Chem. Soc. **114**, 6479 (1992).

²³J. H. B. Chenier, J. A. Howard, J. S. Tse, and B. Mile, J. Am. Chem. Soc. **107**, 7290 (1985).

²⁴H. Bönemann, B. Bogdanović, R. Brinkmann, N. Egeler, R. Benn, I. Topalović, and K. Seevogel, Main Group Met. Chem. **13**, 341 (1990).

²⁵W. E. Rhine, J. Davis, and G. Stucky, J. Am. Chem. Soc. **97**, 2079 (1975).

²⁶C. I. Wu, Y. Hirose, H. Sirringhaus, and A. Kahn, Chem. Phys. Lett. **272**, 43 (1997).